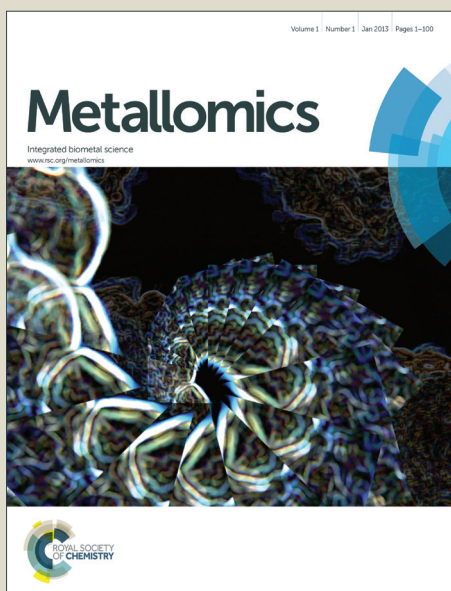


Metallomics

Accepted Manuscript



This is an *Accepted Manuscript*, which has been through the Royal Society of Chemistry peer review process and has been accepted for publication.

Accepted Manuscripts are published online shortly after acceptance, before technical editing, formatting and proof reading. Using this free service, authors can make their results available to the community, in citable form, before we publish the edited article. We will replace this *Accepted Manuscript* with the edited and formatted *Advance Article* as soon as it is available.

You can find more information about *Accepted Manuscripts* in the [Information for Authors](#).

Please note that technical editing may introduce minor changes to the text and/or graphics, which may alter content. The journal's standard [Terms & Conditions](#) and the [Ethical guidelines](#) still apply. In no event shall the Royal Society of Chemistry be held responsible for any errors or omissions in this *Accepted Manuscript* or any consequences arising from the use of any information it contains.

1
2
3
4 1 ***In vitro* evaluation of the cellular influence of indium tin oxide**
5
6 2 **nanoparticles using the human lung adenocarcinoma A549 cells**
7
8
9
10 3

11
12 4 Yosuke Tabei*, Akinari Sonoda, Yoshihiro Nakajima, Vasudevanpillai Biju, Yoji Makita,
13
14
15 5 Yasukazu Yoshida, Masanori Horie
16
17
18 6

19
20
21 7 Health Research Institute, National Institute of Advanced Industrial Science and Technology
22
23 8 (AIST), 2217-14 Hayashi-cho, Takamatsu, Kagawa 761-0395, Japan
24
25
26
27 9

28
29
30 10 *Corresponding author
31

32
33 11 Address: Health Research Institute, National Institute of Advanced Industrial Science and
34
35 12 Technology (AIST), 2217-14 Hayashi-cho, Takamatsu, Kagawa 761-0395, Japan.
36
37

38
39 13 E-mail: y-tabei@aist.go.jp.
40

41
42 14 Tel: +81-87-869-3598
43

44
45 15 Fax: +81-87-869-3553
46
47
48 16
49
50
51
52
53
54
55
56
57
58
59
60

1
2
3
4 **Abstract**
5

6 Indium tin oxide (ITO) is widely used in liquid crystal displays (LCDs) or plasma
7
8 and mobile phone displays. Elevated production and usage of ITO in such displays have
9
10 increased concerns over the safety of industrial workers exposed to particulate aerosols
11
12 produced during cutting, grinding and polishing of these materials. However, the cellular
13
14 influences of ITO nanoparticles (NPs) are still unclear, although it has been reported that
15
16 micro-scale ITO particles induce cytotoxicity. This study aimed to examine the potential of
17
18 ITO NPs to induce cytotoxicity, oxidative stress, and DNA damage using human lung
19
20 adenocarcinoma A549 cells. Here, stable dispersions of a medium containing ITO NPs were
21
22 obtained using pre-adsorption and centrifugal fractionation methods, and the A549 cells were
23
24 incubated in this medium. The ITO NPs had low cytotoxic effects as shown by the WST-1 and
25
26 LDH assay. Transmission electron microscope observation showed cellular uptake of ITO
27
28 NPs. The ITO NPs increased the intracellular level of reactive oxygen species and the
29
30 expression of heme oxygenase 1 gene. Further, the results of alkaline comet assay showed that
31
32 ITO NPs induced DNA damage. Thus, these results suggest that ITO NPs possess a genotoxic
33
34 potential on human lung adenocarcinoma A549 cells.
35
36
37
38
39
40
41
42
43
44
45
46
47
48
49
50
51
52

53 **Key words:** Indium tin oxide, nanoparticle, lung epithelial cell, oxidative stress, genotoxicity,
54
55
56
57
58
59
60

1 Introduction

Indium tin oxide (ITO) is typically a sintered mixture of 90% indium oxide (In_2O_3) and 10% tin oxide (SnO_2). Because of the unique physical properties of ITO, which include high electrical conductivity and transparency, this material is widely used in liquid crystal displays (LCDs) or plasma and mobile phone displays.^{1,2} An increase in the demand for computers and mobile phones had led to a rapid increase in the production of LCDs. Increased production and use of ITO have increased concerns about the safety of industrial workers exposed to particulate aerosols produced during cutting, grinding, and polishing of these materials.

Epidemiological studies and studies of fatal cases of workers exposed to ITO show that ITO induces occupational lung disease and is associated with the risk of interstitial lung damage.^{3,4,5,6,7,8} Lison *et al.*⁹ showed that ITO particles were more toxic than its individual components (In_2O_3 or SnO_2) or the unsintered mixture (In_2O_3 and SnO_2). Their results showed that ITO particles are a novel toxicological materials, which have the potential to generate a high amount of reactive oxygen species (ROS) and induce lung toxicity in experimental animals. ITO particles induce cytotoxicity by cellular uptake of these particles by macrophages and solubilization of indium ion via phagolysosomal acidification.¹⁰ Thus, the Ministry of Health, Labour and Welfare (MHLW) in Japan required a material safety data sheet for indium, set a permissible concentration of $3 \times 10^{-4} \text{ mg m}^{-3}$ for indium compounds,

1 and stated that monitoring of the workplace environment must be conducted every 6
2 months.¹¹

3 A nanoparticle (NP) is defined as a particle that has a diameter in the ranges of 1-100
4 nm (ISO/TS 27678:2008) and has unique physical and chemical properties such as high
5 catalytic activity and distinct absorbance spectrum compared to micro-scale particles.¹² These
6 properties render NPs beneficial for industrial use, and many NPs are used in products
7 familiar to consumers, such as sunscreen and cosmetics. Previous studies have shown
8 size-dependent adverse effects of particles. For example, micro- and nanoscale metal oxide
9 particles such as titanium dioxide (TiO₂), copper oxide (CuO), and nickel oxide (NiO)
10 particles shown different toxicity profiles.^{13,14,15} Therefore, particle size must be important
11 parameter to be considered when evaluating the hazards of ITO particles. Many previous
12 studies have examined the toxicity of micro-scale ITO particles. However, the toxicity caused
13 by ITO NPs has not been examined thus far. We hypothesize that the unique properties of ITO
14 NPs, such as small size and large surface area, may exert biological effects that are quite
15 different from those of micro-scale ITO particles.

16 *In vitro* studies provide important information, especially about the mechanisms
17 underlying NP toxicity.¹⁶ Previous studies have shown that some NPs induce toxic effects
18 such as oxidative stress, apoptosis, cytokine production, and cell death.¹⁷ This study aimed to
19 investigate the cellular influence of ITO NPs using human lung adenocarcinoma A549 cells as

1
2
3
4 1 an *in vitro* model of exposure to ITO NPs via inhalation. In particular, we examined the
5
6
7 2 potential of ITO NPs to cause oxidative stress and DNA damage. Subsequently, we examined
8
9
10 3 the mechanisms underlying these effects. We propose that exposure of A549 cells to ITO NPs
11
12 4 induce ROS production, which may further result in DNA damage.
13
14
15
16
17
18
19
20
21
22
23
24
25
26
27
28
29
30
31
32
33
34
35
36
37
38
39
40
41
42
43
44
45
46
47
48
49
50
51
52
53
54
55
56
57
58
59
60

5

1 **Experimental**

2 **Cell culture**

3 Human lung adenocarcinoma A549 cells (RCB0098) were purchased from RIKEN
4 Bioresource Center (Tsukuba, Ibaraki, Japan). The cells were cultured in Dulbecco's modified
5 Eagle's medium (DMEM; Gibco Life Technologies, Gaithersburg, MD) supplemented with
6 10% heat-inactivated fetal bovine serum (FBS; USDA Tested FBS; ThermoFischer Scientific
7 Inc., Waltham, MA), 100 U mL⁻¹ penicillin, 100 µg mL⁻¹ streptomycin and 250 ng mL⁻¹
8 amphotericin B (Nacalai Tesque Inc., Kyoto, Japan). The DMEM used in this study is referred
9 to as "DMEM-FBS". Cells in DMEM-FBS were placed in 80-cm² flasks (ThermoFischer
10 Scientific Inc.) and cultured at 37°C in an atmosphere of 5% CO₂.

12 **Preparation of ITO-medium dispersions**

13 ITO NPs were purchased from C. I. Kasei Co., Ltd. (Tokyo, Japan) and Xuan Cheng
14 Jing Rui New Material Co., Ltd. (Xuancheng, China). The surface area of the ITO NPs, which
15 were degassed at 120°C for 30 min, was determined with the Quantachrom Autosorb-1
16 instrument by using nitrogen adsorption and the five-point Brunauer-Emmett-Teller (BET)
17 method.

18 For cytotoxicity assays described in Fig. 1, ITO powder was dispersed in 1% BSA at
19 a concentration of 10 mg mL⁻¹ by sonication. Subsequently, the dispersion was diluted with

1 DMEM-FBS at concentrations ranging from 1 to 1000 $\mu\text{g mL}^{-1}$. For other experiments, stable
2 dispersions were prepared using pre-adsorption and centrifugation method¹⁸ with some
3 modification. Briefly, ITO particles were dispersed in 1% BSA at a concentration of 80 mg
4 mL^{-1} by sonication. Subsequently, the dispersion was centrifuged at $4000 \times g$ for 20 min. The
5 precipitated ITO particles were re-dispersed in an equivalent volume of fresh DMEM-FBS.
6 The dispersion was centrifuged at $1000 \times g$ for 20 min. The resulting fraction was applied to
7 A549 cells for evaluating the cellular responses.

9 **Characterization of ITO-medium dispersions**

10 The microstructure of ITO NPs in the ITO-DMEM-FBS dispersion was performed
11 using field-emission scanning electron microscopy (FE-SEM, JSM-6700F; JOEL Ltd., Tokyo,
12 Japan). The secondary particle size in the ITO-DMEM-FBS dispersion was determined using
13 the dynamic light scattering (DLS) particle size analyzer (LB-550; HORIBA Ltd., Kyoto,
14 Japan) at $25.0^\circ\text{C} \pm 0.1^\circ\text{C}$. The light source was a 650-nm laser diode of 5 mW. We determined
15 the particle size using 20-mL samples of ITO-DMEM-FBS dispersion without any
16 pretreatment.

17 The concentrations of components in the medium were determined using inductively
18 coupled plasma atomic emission spectrometry (ICP-AES, SPS7800; Seiko Instruments, Inc.,
19 Tokyo, Japan) and ICP-mass spectrometry (ICP-MS, X-Series II; ThermoFischer Scientific

1
2
3
4 1 Inc.). The ITO-DMEM-FBS dispersion was applied to the ultrafiltration membrane (Amicon
5
6
7 2 Ultra Centrifugal Filters Ultracel 30K; Merck Millipore, Billerica, MA) and centrifuged at
8
9
10 3 $7000 \times g$ for 20 min, and then the concentrations of Na, Ca, P, In, and Sn were determined.
11
12 4 The concentrations of In_2O_3 and SnO_2 included in the stable ITO-DMEM-FBS dispersions
13
14
15 5 were measured using ICP-AES (Thermo Jarrell Ash Corp., Franklin, MA).

16
17
18 6 The ITO particles included in the culture medium were removed by centrifugation at
19
20
21 7 $16,000 \times g$ for 20 min. The supernatant was collected for determination of the protein
22
23
24 8 concentration. The concentration of protein in the culture medium was determined using a
25
26
27 9 protein assay kit from Bio-Rad (Hercules, CA), where BSA was the standard.
28
29
30
31
32

33 **Determination of the viability of cells**

34
35
36 12 Cell viability was examined using the WST-1 solution (Premix WST-1 Cell
37
38
39 13 Proliferation Assay System; Takara Bio, Shiga, Japan). For the WST-1 assay, the cells were
40
41
42 14 seeded in 96-well plates (ThermoFischer Scientific Inc.) at a density of 2×10^5 cells mL^{-1} .
43
44
45 15 The cells were allowed to attach to the plate for approximately 20 h and treated with the
46
47
48 16 ITO-DMEM-FBS dispersion. For the determination of cell viability, the cells were incubated
49
50
51 17 with 10-fold diluted WST-1 solution at 37°C for 1 h. The optical density of formazan was
52
53
54 18 measured at 450 nm using a Tecan Infinite M200 (Tecan Group Ltd., Männedorf,
55
56
57 19 Switzerland).

1
2
3
4 1 To determine whether ITO NPs interfere with the WST-1 reaction product, WST-1
5
6 2 interference test was performed. The cells were seeded in 96-well plates and cultured for 24 h
7
8
9 3 at 37°C in 5% CO₂. The cell culture medium was removed and replaced by 100 μL 10-fold
10
11 4 diluted WST-1 solution. Following an incubation of 1 h at 37°C in 5% CO₂, the optical
12
13 5 density of formazan was measured as described above. Next, 10 μL DMEM-FBS and
14
15 6 ITO-DMEM-FBS dispersions were added to the well and the optical density was determined
16
17
18 7 once more. The result of interference test indicated that the interference of the ITO NPs with
19
20
21 8 WST-1 reaction product was negligible (data not shown).
22
23
24
25
26

27 9 For the lactate dehydrogenase (LDH) assay, the cells were seeded in 12-well plates
28
29
30 10 (ThermoFischer Scientific Inc.) at a density of 2×10^5 cells mL⁻¹. The cells were allowed to
31
32
33 11 attach for approximately 20 h and treated with the ITO-DMEM-FBS dispersion. LDH release
34
35
36 12 was measured with a tetrazolium salt by using Cytotoxicity Detection Kit^{PLUS} (LDH) (Roche
37
38
39 13 Diagnostics GmbH, Mannheim, Germany) according to the manufacturer's protocol. The
40
41
42 14 cytotoxicity was calculated as follows: cytotoxicity (%) = (experimental value – low
43
44
45 15 control)/(high control – low control) × 100. The low control, which refers to spontaneous
46
47
48 16 LDH release, was determined as the LDH released from untreated normal cells. The high
49
50
51 17 control, which refers to the maximum LDH release, was determined as the LDH released
52
53
54 18 from cells that were lysed using the lysis solution provided in the kit.
55
56
57
58
59
60

1 **Transmission electron microscopy**

2 A549 cells incubated in the ITO-DMEM-FBS dispersion were observed using a
3 transmission electron microscope. The cells were incubated in the ITO-DMEM-FBS
4 dispersion for 24 h and then fixed using 1.2% glutaraldehyde for 1 h. The fixed samples were
5 treated with osmium tetroxide (OsO₄) solution for 1 h, dehydrated in ethanol, and embedded
6 in epoxy resin. The resulting samples were then cut into ultrathin sections using a
7 diamond-knife ultramicrotome for examination under a transmission electron microscope.
8 Transmission electron microscopy (TEM) observations were performed using H-7600
9 (Hitachi Corp., Tokyo, Japan). The acceleration voltage was 80.0 kV.

11 **Cellular uptake of ITO NPs**

12 We measured the delivery of ITO NPs to the cell surface and the uptake of NPs by
13 the cells using ICP-MS (ThermoFischer Scientific Inc.). A549 cells in 6-well plates
14 (ThermoFischer Scientific Inc.) were incubated in the ITO-DMEM-FBS dispersion for 24 h,
15 washed with phosphate buffered saline (PBS) three times to remove loosely bound ITO NPs
16 on the cell surface, and detached using 0.25% trypsin. The cell pellet was resuspended in 1
17 mL PBS, and the number of cells was counted using a hemocytometer. The cells were mixed
18 with acid solution (water:nitric acid:hydrochloric acid = 4:1:3) and then heated at 80°C for 2 h
19 to dissolve the cellular contents. The solutions were diluted with water and used for ICP-MS

1 analysis.

2

3 **Measurement of the level of intracellular ROS**

4 The level of intracellular ROS was detected using 2',7'-dichlorodihydrofluorescein
5 diacetate (DCFH-DA) (Sigma-Aldrich, St. Louis, MO). DCFH-DA was dissolved in DMSO
6 at 5 mM as a stock solution and stored at -20°C. After incubation of cells with the
7 ITO-DMEM-FBS dispersion, the medium was changed to a serum-free DMEM containing 10
8 µM of DCFH-DA, and the cells were incubated for 30 min at 37°C. Then, cells were washed
9 once with PBS, collected by 0.25% trypsinization, washed again with PBS, and resuspended
10 in 500 µL of PBS. Cell samples in PBS were excited with a 488-nm argon laser in the
11 FACSCalibur flow cytometer (Becton, Dickinson and Company, Franklin Lakes, NJ). The
12 emission of DCF was recorded at 525 nm. Data were collected from at least 5000 gated
13 events.

14

15 **Isolation of total RNA and quantitative real-time polymerase chain reaction analysis**

16 For isolation of total RNA, the cells were cultured in 6-well plates (ThermoFischer
17 Scientific Inc.) and incubated in the ITO-DMEM-FBS dispersion for 24 and 72 h.
18 Subsequently, total RNA was extracted using the RNeasy mini kit (Qiagen, Valencia, CA)
19 according to the manufacturer's instructions. The concentration of the RNA was determined

1 using a Nanodrop ND-1000 spectrophotometer (ThermoFischer Scientific Inc.). The first
2 strand cDNA was synthesized from 0.5 μg of total RNA by using the SuperScript VILO
3 cDNA synthesis kit (Invitrogen, Carlsbad, CA) according to the manufacturer's instructions.
4 The mRNA levels of heme oxygenase 1 (*HMOX-1*) were analyzed using the TaqMan gene
5 expression assay (IDs: HMOX-1, Hs01110250_m1, Applied Biosystems). The housekeeping
6 gene β -actin (Assay ID: Hs99999903_m1) was used as an internal control. The levels of each
7 target mRNA were measured using the Applied Biosystems 7300 Real Time PCR System.
8 The cyclor conditions were as follows: 2 min at 50°C, 10 min at 95°C, and 60 cycles each of
9 15 s at 95°C and 1 min at 60°C. The mRNA expression levels of *HMOX-1* in each sample
10 were normalized to the β -actin mRNA levels and were then compared with those of the
11 untreated controls. The results are reported as fold change over control.

12

13 **Alkaline comet assay**

14 An alkaline comet assay was performed according to the instructions provided by the
15 manufacturer (Comet Assay; Trevigen, Gaithersburg, MD). For the comet assay, the cells ($2 \times$
16 10^5 cells mL^{-1}) were seeded into 6-well plates. After overnight incubation, the cells were
17 exposed to the ITO-DMEM-FBS dispersion for 24 and 72 h. Then, the cells were washed and
18 resuspended in Ca^{2+} - and Mg^{2+} -free PBS solution. The cell suspension (1×10^5 cells mL^{-1})
19 was mixed with LMagarose at a ratio of 1:10 (v/v). This mixture was immediately transferred

1 onto the CometSlide (Trevigen). The cells were lysed overnight at 4°C; then the CometSlides
2 were transferred to fresh dishes containing cold alkaline unwinding solution (0.2 M NaOH
3 and 1 mM EDTA, pH > 13) and incubated for 60 min at 4°C for the DNA unwinding step.
4 The CometSlides were placed on a horizontal electrophoresis unit and the unit was filled with
5 fresh buffer (0.2 M NaOH, 1 mM EDTA, pH > 13) to cover the CometSlides. Electrophoresis
6 was performed at 20 V for 35 min at 4°C in the dark and then staining was performed with a
7 silver staining kit (Trevigen). The comet tail length was defined as the distance between the
8 leading edge of the nucleus and the end of the tail. At least 50 comet tail lengths/slide were
9 quantified from three independent experiments performed in duplicate.

10

11 **Clonogenic assay**

12 The colony-forming ability (i.e., cell proliferation) was detected using a clonogenic
13 assay based on the methods described by Herzog *et al.*¹⁹ and Franken *et al.*²⁰ Briefly, the cells
14 were seeded in 6-well plates (ThermoFischer Scientific Inc.) at a density of 300 cells/well.
15 Each well contained 2 mL of the cell culture medium. The cells were allowed to attach for 20
16 h and treated with 2 mL of the ITO-DMEM-FBS dispersion. Then, the cells were cultured for
17 the time period required for the control cells to form colonies (one colony was defined as ≤ 50
18 cells), i.e., 7 days. Subsequently, the dispersions were removed and cells washed with 2 mL
19 PBS. After fixation with 100% methanol for 20 min, the cells were stained with Giemsa's

1 staining solution (Kanto Chemical Co., Inc., Tokyo, Japan) for 20 min and rinsed with
2 distilled water. The number of colonies was counted.

3

4 **Statistical analysis**

5 Data are mean \pm standard deviation values from at least three independent
6 experiments. Statistical analyses were performed with the analysis of variance (ANOVA) by
7 using Dunnett test for multiple comparisons.

8

1 **Results**

2 **Cellular influences of un-fractionated ITO-medium dispersion**

3 We used three kinds of ITO NPs in this study (Table 1). The ITO NPs were dispersed
4 in 1% BSA at a concentration of 10 mg mL⁻¹ by sonication. Subsequently, the dispersion was
5 diluted with DMEM-FBS at concentrations ranging from 1 to 1000 µg mL⁻¹, and then, the
6 A549 cells were incubated in the dispersions. After incubation for 6 and 24 h, we examined
7 the cell viability and cell membrane damage by using WST-1 assay and LDH assay,
8 respectively. The cell viability was not influenced by ITO exposure even at ITO
9 concentrations of 1.0 mg mL⁻¹ (Fig. 1A). The cell viability did not decrease despite prolonged
10 exposure (7 days) to ITO (data not shown). In addition, no cell membrane damage was
11 observed in the A549 cells exposed to ITO (Fig. 1B).

12 The ITO dispersion included large secondary particles that were extremely unstable.
13 Since the large secondary particles accumulated on the cells by gravity sedimentation, the
14 concentration of the dispersion did not reflect the concentration to which the cells were
15 exposed. Previous studies showed that stability of the dispersion is important for evaluating
16 the cellular responses of NPs.^{21,22} Therefore, further cellular responses were examined by
17 using a stable ITO-DMEM-FBS dispersion.

18 19 **Characterization of fractionated ITO-DMEM-FBS dispersion**

1 The stable dispersion was prepared by pre-adsorption and centrifugal fractionation
2 methods as reported previously.¹⁸ Examination of primary ITO particles by using FE-SEM
3 showed that most ITO NPs were globular particles (Fig.2A). The average sizes of ITO NPs in
4 sample A, sample B, and sample C were 20.8, 28.6, and 31.0 nm, respectively; the sizes were
5 calculated from the diameters measured for 100 particles (Fig. 2B).

6 The size of secondary ITO NPs in the dispersion was measured using DLS (Fig. 3A).
7 The sizes of the secondary particle in sample A, sample B, and sample C based on particle
8 numbers were 106.3, 63.4, and 57.3 nm, respectively, and those based on light scattering
9 intensities were 206.2, 128.1, and 130.7 nm, respectively. Although the sizes of secondary
10 particles in sample A gradually increased, those of particles in sample B and sample C did not
11 change during the experimental period. Further, we examined the stability of the dispersion
12 using DLS (Fig. 3B). The DLS results suggested that slight sedimentation occurred in sample
13 A and sample B, but we did not observe a marked decrease in the light scattering intensity.
14 Sample C did not show a significant change in the light scattering intensity for 4 days after
15 preparation. These results indicated that the ITO-DMEM-FBS dispersions prepared in this
16 study were suitable for *in vitro* experiments.

17 Results of the characterization of the ITO-DMEM-FBS dispersion are shown in
18 Table 1. The concentration of In₂O₃ in sample A, sample B, and sample C were 720, 490, and
19 480 μg mL⁻¹, respectively. The concentrations of SnO₂ in the sample A, sample B, and sample

1
2
3
4 1 C were 70, 50, and 50 $\mu\text{g mL}^{-1}$, respectively. The release of soluble indium and tin from ITO
5
6
7 2 NPs into the medium was very small. The slight decrease in the concentrations of sodium and
8
9
10 3 calcium and an increase in the concentration of phosphorus and protein in the ITO medium
11
12 4 dispersion did not have marked effects. These results indicated that the ITO NPs did not affect
13
14
15 5 the composition of the medium.
16
17
18
19
20
21
22
23

7 **Influence of the stable ITO-DMEM-FBS dispersion on cell viability and cell membrane**

8 The influence of ITO NPs on cell viability was examined using stable
9 ITO-DMEM-FBS dispersions prepared in the above step (Fig. 4). We found that the inhibitory
10 effect of ITO NPs on the cell viability were not remarkable, although the viability was slightly
11 inhibited at 72 h. Further, we measured the cell membrane integrity after incubation with the
12 stable ITO-DMEM-FBS dispersion for 6, 24, and 72 h (Fig. 5). We did not observe a
13 significant cytotoxic effect at all the tested concentrations.
14

15 **Uptake of ITO NPs by A549 cells.**

16 A549 cells were incubated with the ITO-DMEM-FBS dispersion for 24 h, and then,
17 the uptake of ITO NPs by the A549 cells was determined using TEM and by ICP-MS (Fig. 6).
18 TEM images showed that ITO NPs were incorporated into the A549 cells after 24 h
19 incubation (Fig.6A). Internalized ITO NPs existed in a lysosome-like structure in the

1 cytoplasm. We did not observe translocation of ITO NPs into the nucleus. We measured the
2 amounts of internalized ITO NPs in the A549 cells by using ICP-MS (Fig. 6B). After
3 incubating the cells with the ITO-DMEM-FBS dispersion for 24 h, the entire cell population
4 was detached and the cells were lysed and analyzed to determine the concentration of
5 internalized indium. ICP-MS measurements showed that the amount of indium uptake
6 correlated with the concentration of ITO NPs in the extracellular solution.

8 **Effects of stable ITO-DMEM-FBS dispersion on oxidative stress**

9 Previous studies indicated that NP-mediated cytotoxicity is associated with ROS
10 production.^{23,24,25,26} Thus, we examined the effect of ITO NPs on oxidative stress. The stable
11 ITO-DMEM-FBS dispersions were exposed to A549 cells for 6, 24, and 72 h; subsequently,
12 we measured the intracellular ROS levels using the fluorescent dye DCFH-DA, which shows
13 enhanced fluorescence in the presence of oxidative stress (Fig. 7A). After 24 h exposure to
14 ITO NPs, a significant increase in ROS production was observed for sample B and sample C.
15 The A549 cells exposed to sample A showed a significant increase of ROS production at 72 h
16 in a concentration-dependent manner. Our results showed that exposure of A549 cells to
17 ITO-DMEM-FBS dispersion causes an increase in ROS generation reflected by an increase in
18 DCF fluorescence.

19 We measured the mRNA levels of *HMOX-1*, a marker of oxidative stress, to

1
2
3
4 1 determine the oxidative stress response of A549 cells exposed to the ITO-DMEM-FBS
5
6 2 dispersion (Fig. 8). The mRNA levels of *HMOX-1* gradually induced after incubation with the
7
8
9 3 ITO-DMEM-FBS dispersion. This up-regulation of *HMOX-1* mRNA was prominent at 72 h.
10
11
12 4 These results suggested that ITO NPs induced oxidative stress.
13
14
15
16
17

18 **DNA damage and colony-forming ability of A549 cells incubated with the stable**
19
20
21 **ITO-DMEM-FBS dispersion**
22
23

24 8 We examined the DNA single-strand breaks by using the alkaline comet assay. Here,
25
26
27 9 A549 cells were incubated with the stable ITO-DMEM-FBS dispersion as described in the
28
29
30 10 Experimental section. The representative images of DNA damage obtained using the alkaline
31
32
33 11 comet assay of A549 cells exposed to ITO NPs are shown in Fig. 9. The ITO NPs induced
34
35
36 12 DNA strand breakages at 24 h. The lesions were permanently induced in cells exposed sample
37
38
39 13 B and sample C. The tail length of cells exposed to sample B and sample C increased 2.9- and
40
41
42 14 2.6-fold, respectively, compared to that of the untreated cells at 72 h. Conversely, when cells
43
44
45 15 were exposed to sample A, the length of comet tail decreased at 72 h.
46

47 16 The influence of ITO NPs on cell proliferation was examined using a clonogenic
48
49
50 17 assay (Fig. 10). The results of the clonogenic assay showed a concentration-dependent
51
52
53 18 decrease in colony-forming ability for two out of the three samples, i.e., sample B and sample
54
55
56 19 C. Incubation with sample A induced a statistically significant but not a
57
58
59
60

1
2
3
4 1 concentration-dependent inhibition of colony formation.
5
6
7 2
8
9
10
11
12
13
14
15
16
17
18
19
20
21
22
23
24
25
26
27
28
29
30
31
32
33
34
35
36
37
38
39
40
41
42
43
44
45
46
47
48
49
50
51
52
53
54
55
56
57
58
59
60

1 Discussion

2 Owing to the wide-spread use of ITO, it has become important to investigate the
3 possible adverse effects of ITO on human health and the environment. Since inhalation is a
4 significant route of exposure to ITO NPs, we examined the effect of ITO NPs on human lung
5 adenocarcinoma A549 cells, a model cell line for lung exposure. In this study, we investigated
6 the possible hazards of exposure to a range of ITO NPs with respect to cytotoxicity, induction
7 of oxidative stress, and DNA damage. The results of the cytotoxicity assays (WST-1 and LDH
8 assays) showed that the ITO NPs had low acute toxic effects on the A549 cells. The results of
9 the genotoxicity assay (comet assay) showed severe DNA strand breaks in the A549 cells
10 exposed to ITO NPs.

11 Cellular uptake of NPs is an important process that governs the cellular effects of
12 NPs. Cellular uptake of NPs mediated by different processes, including phagocytosis²⁷ and
13 endocytosis.^{28,29} Several studies have indicated that, since the uptake of ITO particles via
14 macrophages is more efficient than that via epithelial cells, ITO particles are cytotoxic to
15 macrophages but not to epithelial cells.^{9,10} However, our results show that the ITO NPs are
16 internalized within the intracellular space in the A549 cells (Fig. 6A) and induce intracellular
17 oxidative stress (Fig. 7). The differences in the results of previous studies and those of our
18 study may be due to the size of ITO particles. Previous toxicological studies were performed
19 using micro-scale ITO particles. In this study, we examined the cellular effects of ITO NPs,

1 which consist of nanoscale primary and secondary particles. Recent studies showed that the
2 cellular uptake of particles is size-dependent.^{30,31} The intracellular concentrations of indium
3 were correlated with extracellular ITO concentrations (Fig. 6B). Moreover, the sizes of
4 secondary particles in sample B and sample C were smaller than those of the particles in
5 sample A, and thus sample B and sample C showed higher genotoxicity (Fig. 9). Therefore,
6 although the mechanism underlying the cellular uptake of ITO NPs is unclear, our results
7 showed that ITO NPs were taken up by the A549 cells, and they induced oxidative stress and
8 DNA damage.

9 The stability of the NP dispersion medium is important for *in vitro* evaluation of
10 NPs.^{21,22} While smaller particles reach the cells by diffusion, larger particles reach by gravity
11 sedimentation. Thus, the concentration of the dispersion is not the concentration to which the
12 cell is exposed. In this study, the secondary ITO particles of in DMEM-FBS were very stable
13 (Fig. 3). Neither the particle size nor the light scattering intensity changed during the
14 experiment period. Therefore, the cellular responses evaluated in this study were not
15 influenced by large sedimentation, and the concentrations of ITO in the dispersion accurately
16 reflected the concentration of cellular exposure.

17 The release of metal ions is an important factor associated with the cytotoxicity of
18 metal oxide NPs.^{15,32} For example, high cytotoxicity of CuO NPs is associated with the
19 release of copper ions from the internalized CuO NPs.³³ Moreover, while NiO and chromium

1
2
3
4 1 oxide (Cr_2O_3) NPs easily dissolve in the culture medium and induce marked oxidative stress,
5
6
7 2 their micro-scale particles do not dissolve in the medium.^{15,34} ITO is insoluble at
8
9
10 3 physiological pH.⁶ The ITO NPs used in this study did not release large amounts of indium
11
12
13 4 ion into the medium (Table 1). Thus, the cellular effects of ITO NPs are different from those
14
15
16 5 of degradable NPs such as CuO, NiO and Cr_2O_3 . Previous studies have shown that the
17
18
19 6 adsorption ability influences the cellular effects of NPs, especially of the insoluble NPs.^{35,36}
20
21
22 7 TiO_2 , cerium oxide (CeO_2) and zinc oxide (ZnO) NPs have strong adsorption ability; thus,
23
24
25 8 these NPs adsorbed the proteins and calcium ions in the medium thereby depleting the
26
27
28 9 medium of these components. In this study, we prepared a stable ITO-DMEM-FBS dispersion
29
30
31 10 by using pre-adsorption and centrifugation method to prevent indirect toxicity by medium
32
33
34 11 depletion. The concentrations of the medium components such as sodium, calcium, and
35
36
37 12 phosphorus were not affected by the ITO NPs (Table 1). Therefore, the cellular effects
38
39
40 13 observed in our study were not influenced by medium depletion and were induced by the ITO
41
42
43 14 NPs alone.

44
45
46 15 Several studies have indicated that oxidative stress is frequently associated with NP
47
48
49 16 toxicity.^{17,37} Oxidative stress induces a wide variety of physiological and cellular effects
50
51
52 17 including inflammation, DNA damage, and apoptosis.^{23,24,25,26} Moreover, studies on
53
54
55 18 indium-containing compounds suggest that the production of ROS is the mechanism
56
57
58 19 underlying NP-induced toxicity.^{9,38} We hypothesized that the cellular effects induced by ITO

1 NPs in our studies were also mediated by the generation of oxidative stress. However, the
2 results of the intracellular ROS level (Fig. 7) were not correlated with the generation of DNA
3 damage (Fig. 9). Although the reasons of the difference remain unclear, the expression of
4 *HMOX-1* may be attributed to this differences. The induction of *HMOX-1* provides protection
5 against oxidative stress, chemical toxicity and certain chronic disorders.³⁹ In sample B and
6 sample C, the generation of ROS was observed at an early stages (< 24 h) (Fig. 7B and C), but
7 the expression of *HMOX-1* was not induced at 24 h (Fig. 8B and C). In sample A, the
8 intracellular ROS level increased after long-term exposure (72 h) (Fig. 7A). The expression of
9 *HMOX-1* was sufficiently induced at this time point (Fig. 8A). Therefore, our results suggest
10 that ITO NPs induced genotoxicity by generation of ROS, which were not neutralized by
11 antioxidant-related enzymes. Besides the generation of ROS, the impairment of the DNA
12 repair enzyme may be involved in the accumulation of DNA damage. Previously, it was
13 demonstrated that the activity of DNA repair enzyme was inhibited by the exposure of
14 indium.⁴⁰ Martin *et al.* demonstrated that the addition of hydroxyurea (HU) and cytosine
15 arabinoside (Ara-C) enhanced the sensitivity of the comet assay in response to certain
16 genotoxins.⁴¹ This analysis is based on the accumulation of single-strand breaks during the
17 DNA repair process. Thus, the inhibitory effect of ITO NPs on the excision repair process will
18 be elucidated by performing the comet assay in the presence of HU and Ara-C.

19 In this study, we investigated that cellular influences of ITO NPs and demonstrated

1
2
3
4 1 that ITO NPs have genotoxic effect on A549 cells. However, it is difficult to predict biological
5
6
7 2 responses to low-dose environmental exposures based on adverse effects induced by
8
9
10 3 high-dose concentrations. Recently, it was reported that Fourier-transform infrared
11
12
13 4 spectroscopy is useful to detect alterations induced by carbon NPs at environmentally relevant
14
15
16 5 concentrations.^{42,43} Such studies will provide some insights into ITO-induced toxic
17
18
19 6 mechanisms at environmentally relevant exposure levels. Further, the precise cellular
20
21
22 7 signaling mechanisms underlying NP-mediated toxicity remains unclear. Therefore, further
23
24
25 8 studies are required to clarify the mechanisms underlying the cellular uptake and genotoxicity
26
27
28 9 of ITO NPs.

29
30
31
32
33
34
35
36
37
38
39
40
41
42
43
44
45
46
47
48
49
50
51
52
53
54
55
56
57
58
59
60

1
2
3
4 **1 Conclusion**
5

6
7 2 Our results showed that, similar to other NPs, ITO NPs were taken up into the
8
9
10 3 cultured human lung adenocarcinoma A549 cells. Furthermore, the ITO NPs possess potential
11
12 4 for inducing DNA damage in lung epithelial cells, which may be mediated through oxidative
13
14
15 5 stress. To our knowledge, this is the first study to report the toxic effects of ITO NPs on
16
17
18 6 human lung epithelial cells. The cellular effects of ITO NPs evaluated by *in vitro* experiments
19
20
21 7 may provide some insights into indium-induced lung disease.
22
23
24 8

1
2
3
4 **1 Acknowledgements**
5

6
7 2 The authors are thankful to Ms. Emiko Kobayashi, Bioproduction Research Institute,
8
9 3 National Institute of Advanced Industrial Science and Technology (AIST) for carrying out the
10
11
12 4 transmission electron microscopy.
13
14

15
16 5

17
18 **6 Conflict of interest**
19

20
21 7 The authors declare that there are no conflicts of interest.
22
23 8
24
25
26
27
28
29
30
31
32
33
34
35
36
37
38
39
40
41
42
43
44
45
46
47
48
49
50
51
52
53
54
55
56
57
58
59
60

1
2
3
4 **References**

- 5
6
7 1. U. Betz, M. Kharrazi Olsson, J. Marthy, M. F. Escolá and F. Atamny, *Surf. Coat. Technol.*
8
9 2006, **200**, 5751.
- 10
11
12 2. V. Fthenakis, *Renew. Sustain. Energy Rev.*, 2009, **13**, 2746.
- 13
14
15 3. T. Homma, T. Ueno, K. Sekizawa, A. Tanaka and M. Hirata, *J. Occup. Health*, 2003, **45**,
16
17 137-139.
- 18
19
20
21 4. S. Homma, A. Miyamoto, S. Sakamoto, K. Kishi, N. Motoi and K. Yoshimura, *Eur.*
22
23 *Respir. J.*, 2005, **25**, 200.
- 24
25
26
27 5. T. Chonan, O. Taguchi and K. Omae, *Eur. Respir. J.*, 2007, **29**, 317.
- 28
29
30 6. T. Hamaguchi, K. Omae, T. Takebayashi, Y. Kikuchi, N. Yoshioka, Y. Nishiwaki, A.
31
32 Tanaka, M. Hirata, O. Taguchi and T. Chonan, *Occup. Environ. Med.*, 2008, **65**, 51.
- 33
34
35 7. M. Nakano, K. Omae, A. Tanaka, M. Hirata, T. Michikawa, Y. Kikuchi, N. Yoshioka, Y.
36
37 Nishiwaki and T. Chonan, *J. Occup. Health*, 2009, **51**, 513.
- 38
39
40
41 8. K. J. Cummings, W. E. Donat, D. B. Etensohn, V. L. Roggli, P. Ingram and K. Kreiss,
42
43 *Am. J. Respir. Crit. Care Med.*, 2010, **181**, 458.
- 44
45
46
47 9. D. Lison, J. Laloy, I. Corazzari, J. Muller, V. Rabolli, N. Panin, F. Huaux, I. Fenoglio and
48
49 B. Fubini, *Toxicol. Sci.*, 2009, **108**, 472.
- 50
51
52
53 10. W. M. Gwinn, W. Qu, C. J. Shines, R. W. Bousquet, G. J. Taylor, M. P. Waalkes and D. L.
54
55 Morgan, *Toxicol. Sci.*, 2013, **135**, 414.
- 56
57
58
59
60

- 1
2
3
4 11. Ministry of Health, Labour and Welfare, 2010, Japan, No. 1222-3.
5
6
7 12. G. Oberdörster, E. Oberdörster and J. Oberdörster, *Environ. Health Perspect.*, 2005, **113**,
8
9 823.
10
11
12 13. S. Q. Li, R. R. Zhu, H. Zhu, X. Y. Xue, X. Y. Sun, S. D. Yao and S. L. Wang, *Food Chem.*
13
14
15 *Toxicol.*, 2008, **46**, 3626.
16
17
18 14. H. L. Karlsson, J. Gustafsson, P. Cronholm and L. Möller, *Toxicol. Lett.*, 2009, **188**, 112.
19
20
21 15. M. Horie, K. Nishio, K. Fujita, H. Kato, A. Nakamura, S. Kinugasa, S. Endoh, A.
22
23
24 Miyachi, K. Yamamoto, H. Murayama, E. Niki, H. Iwahashi, Y. Yoshida and J.
25
26
27 Nakanishi, *Chem. Res. Toxicol.*, 2009, **22**, 1415.
28
29
30 16. M. Horie, H. Kato, K. Fujita, S. Endoh and H. Iwahashi, *Chem. Res. Toxicol.*, 2012, **25**,
31
32
33 605.
34
35
36 17. A. Nel, T. Xia, L. Mädler and N. Li, *Science*, 2006, **311**, 622.
37
38
39 18. M. Horie, K. Nishio, K. Fujita, H. Kato, S. Endoh, M. Suzuki, A. Nakamura, A. Miyachi,
40
41
42 S. Kinugasa, K. Yamamoto, H. Iwahashi, H. Murayama, E. Niki and Y. Yoshida, *Toxicol.*
43
44
45 *In Vitro*, 2010, **24**, 1629.
46
47
48 19. E. Herzog, A. Casey, F. M. Lyng, G. Chambers, H. J. Byrne and M. Davoren, *Toxicol.*
49
50
51 *Lett.*, 2007, **174**, 49.
52
53
54 20. N. A. Franken, H. M. Rodermond, J. Stap, J. Haveman and C. van Bree, *Nat. Protoc.*,
55
56
57 2006, **1**, 2315.
58
59
60

- 1
2
3
4 1 21. J. G. Teeguarden, P. M. Hinderliter, G. Orr, B. D. Thrall and J. G. Pounds, *Toxicol. Sci.*,
5
6
7 2 2007, **95**, 300.
8
9
10 3 22. H. Kato, M. Suzuki, K. Fujita, M. Horie, S. Endoh, Y. Yoshida, H. Iwahashi, K.
11
12 4 Takahashi, A. Nakamura and S. Kinugasa, *Toxicol. In Vitro.*, 2009, **23**, 927.
13
14
15 5 23. P. V. AshaRani, G. Low Kah Mun, M. P. Hande and S. Valiyaveetil, *ASC Nano*, 2009, **3**,
16
17 6 279.
18
19
20
21 7 24. Y. H. Hsin, C. F. Chen, S. Huang, T. S. Shin, P. S. Lai and P. J. Chueh, *Toxicol. Lett.*, 2008,
22
23 8 **179**, 130.
24
25
26
27 9 25. J. Ahmad, M. Ahamed, M. J. Akhtar, S. A. Alrokayan, M. A. Siddiqui, J. Musarrat and A.
28
29 10 A. Al-Khedhairi, *Toxicol. Appl. Pharmacol.*, 2012, **259**, 160.
30
31
32
33 11 26. I. Passagne, M. Morille, M. Rousset, I. Pujalte and B. L'Azou, *Toxicology*, 2012, **299**,
34
35 12 112.
36
37
38 13 27. R. Weissleder, H. C. Cheng, A. Bogdanova and A. Bogdanov, *J. Magn. Reson. Imaging*,
39
40 14 1997, **7**, 258.
41
42
43
44 15 28. U. Schoepf, E. Marecos, R. Melder, R. Jain and R. Weissleder, *BioTechniques*, 1998, **24**,
45
46 16 642.
47
48
49
50 17 29. A. Moore, J. P. Basilion, E. A. Chiocca and R. Weissleder, *Biochim. Biophys. Acta*, 1998,
51
52 18 **1402**, 239.
53
54
55
56 19 30. F. Lu, S. H. Wu, Y. Hung and C. Y. Mou, *Small*, 2009, **5**, 1408.
57
58
59
60

- 1
2
3
4 1 31. P. O. Andersson, C. Lejon, B. Ekstrand-Hammarström, C. Akfur, L. Ahlinder, A. Bucht
5
6
7 2 and L. Österlund, *Small*, 2011, **7**, 514.
8
9
10 3 32. H. L. Karlsson, P. Cronholm, J. Gustafsson and L. Möller, *Chem. Res. Toxicol.*, 2008, **21**,
11
12 4 1726.
13
14
15 5 33. A. M. Studer, L. K. Limbach, L. Van Duc, F. Krumeich, E. K. Athanassiou, L. C. Gerber,
16
17
18 6 H. Moch and W. J. Stark, *Toxicol. Lett.*, 2010, **197**, 169.
19
20
21 7 34. M. Horie, K. Nishio, S. Endoh, H. Kato, K. Fujita, A. Miyauchi, A. Nakamura, S.
22
23
24 8 Kinugasa, K. Yamamoto, E. Niki, Y. Yoshida and H. Iwahashi, *Environ. Toxicol.*, 2013,
25
26
27 9 **28**, 61.
28
29
30 10 35. A. Casey, E. Herzog, F. M. Lyng, H. J. Byrne, G. Chambers and M. Davoren, *Toxicol.*
31
32
33 11 *Lett.*, 2008, **179**, 78.
34
35
36 12 36. M. Horie, K. Nishio, K. Fujita, S. Endoh, A. Miyauchi, Y. Saito, H. Iwahashi, K.
37
38
39 13 Yamomoto, H. Murayama, H. Nakano, N. Nanashima, E. Niki and Y. Yoshida, *Chem. Res.*
40
41
42 14 *Toxicol.*, 2009, **22**, 543.
43
44
45 15 37. Y. Ju-Nam and J. R. Lead, *Sci. Total Environ.*, 2008, **400**, 396.
46
47
48 16 38. H. H. Liu, C. Y. Chen, G. I. Chen, L. H. Lee and H. L. Chen, *Int. Arch. Occup. Environ.*
49
50
51 17 *Health*, 2012, **85**, 447.
52
53
54 18 39. A. K. Jaiswal, *Free Radic. Biol. Med.*, 2004, **11**, 549.
55
56
57 19 40. J. Bustamante, L. Dock, M. Vahter, B. Fowler, and S. Orrenius, *Toxicology*, 1997, **118**,

1 129.

2 41. F. L. Martin, K. J. Cole, M. H. Orme, P. L. Grover, D. H. Phillips, and S. Venitt, *Mutat.*

3 *Res.*, 1999, **445**, 21.

4 42. J. Li, R. Strong, J. Trevisan, S. W. Fogarty, N. J. Fullwood, K. C. Jones and F. L. Martin,

5 *Environ. Sci. Technol.*, 2013, **47**, 10005.

6 43. M. J. Riding, J. Trevisan, C. J. Hirschmugl, K. C. Jones, K. T. Semple and F. L. Martin,

7 *Environ. Int.*, 2012, **50**, 56.

8

1 **Table**2 **Table 1** Characterization of the ITO–DMEM–FBS dispersion used in this study.

Sample	Primary particle size ^a (nm)	Specific surface area (m ² g ⁻¹)	Secondary particle size ^b (nm)	Metal oxide conc. (μg mL ⁻¹)	Soluble metal conc. (μM)	Protein conc. (mg mL ⁻¹)	Salt composition of the dispersion		
							Na (mM)	Ca (mM)	P (μM)
A	30	30.8	<i>d_l</i> : 206.2 <i>d_n</i> : 106.3	In ₂ O ₃ : 720 SnO ₂ : 70	In: 0.03 Sn: 1.80	3.4	144.7	0.8	86.6
B	30	16.0	<i>d_l</i> : 128.1 <i>d_n</i> : 63.4	In ₂ O ₃ : 490 SnO ₂ : 50	In: 0.08 Sn: 0.14	5.1	155.3	1.3	69.6
C	30	15.3	<i>d_l</i> : 130.7 <i>d_n</i> : 57.3	In ₂ O ₃ : 480 SnO ₂ : 50	In: 0.07 Sn: 0.18	4.1	146.3	1.3	87.8
DMEM-FBS					In: 0.02 Sn: 0.00	3.4	170.6	1.9	66.1

3 ^aAccording to manufacture's data sheet4 ^b*d_l* and *d_n* mean secondary particle size based on the light scattering intensity and particle
5 number, respectively.

6

1
2
3
4 **1 Figure legends**

5
6 **2 Fig. 1** Effects of un-fractionated indium tin oxide (ITO) NPs on cell viability and the cell
7
8
9
10
11
12
13
14
15
16
17
18
19
20
21
22
23
24
25
26
27
28
29
30
31
32
33
34
35
36
37
38
39
40
41
42
43
44
45
46
47
48
49
50
51
52
53
54
55
56
57
58
59
60

3 membrane. (A) Effect of ITO-DMEM-FBS dispersion on cell viability. A549 cells were
4 incubated with ITO-DMEM-FBS dispersions for 6 and 24 h. The cell viability was measured
5 using the WST-1 assay, and results were given as percent related to untreated controls. (B)
6 Effect of the ITO-DMEM-FBS dispersion on cell membrane damage. A549 cells were
7 incubated with ITO-DMEM-FBS dispersions for 6 and 24 h, and then, cell membrane damage
8 was determined by measuring the intracellular release of LDH. The method of calculating
9 cytotoxicity is described in the Experimental section. No significant differences were
10 observed between the untreated cells and ITO-exposed cells (Dunnett, analysis of variance
11 [ANOVA]).

12
13 **Fig.2** Size distributions of indium tin oxide (ITO) NPs. (A) Field-emission scanning electron
14
15
16
17
18
19
20
21
22
23
24
25
26
27
28
29
30
31
32
33
34
35
36
37
38
39
40
41
42
43
44
45
46
47
48
49
50
51
52
53
54
55
56
57
58
59
60

microscopy (FE-SEM) observation of ITO NPs in stable ITO-DMEM-FBS dispersions. (B)
Histograms of the particle size distribution of ITO NPs.

17 **Fig. 3** Stabilities of ITO-DMEM-FBS dispersions. (A) ITO secondary particle sizes (d) based
18
19
20
21
22
23
24
25
26
27
28
29
30
31
32
33
34
35
36
37
38
39
40
41
42
43
44
45
46
47
48
49
50
51
52
53
54
55
56
57
58
59
60

on particle number (open circles) and based on light scattering intensities (closed circles) were
measured using dynamic light scattering (DLS). (B) Light scattering intensities of ITO

1 secondary particles were measured by DLS. A plot of relative light scattering intensities of
2 ITO secondary particles versus time (day). The ITO-DMEM-FBS dispersions were prepared
3 at day 0.

4
5 **Fig. 4** Effect of stable ITO-DMEM-FBS dispersions on cell viability. A549 cells were
6 exposed to ITO-DMEM-FBS dispersions for 6, 24, and 72 h. The cell viability was measured
7 using the WST-1 assay, and the results were given as percent related to untreated controls. **
8 $P < 0.01$ (versus control, Dunnett, analysis of variance [ANOVA]).

9
10 **Fig. 5** Effect of stable ITO-DMEM-FBS dispersions on the cell membrane. A549 cells were
11 exposed to ITO-DMEM-FBS dispersions for 6, 24, and 72 h, and then, cell membrane
12 damage was determined by measuring the intracellular LDH release. The method of
13 calculating cytotoxicity is described in the Experimental section. No significant differences
14 were observed between untreated cells and ITO-exposed cells (Dunnett, analysis of variance
15 [ANOVA]).

16
17 **Fig. 6** Cellular uptake of indium tin oxide (ITO) NPs by A549 cells. (A) Examination of A549
18 cells incubated with the ITO-DMEM-FBS dispersions under the transmission electron
19 microscope. The A549 cells were incubated with the ITO-DMEM-FBS dispersions for 24 h.

1 Overview of the cell (left) and details of the part in white frames (right). The concentrations
2 of indium oxide (In_2O_3) in sample A, sample B, and sample C were 720, 490, and 480 μg
3 mL^{-1} , respectively. (B) Internal concentrations of indium obtained by inductively coupled
4 plasma mass spectrometry (ICP-MS). The A549 cells were incubated with the
5 ITO-DMEM-FBS dispersion for 24 h, and then, the intracellular concentrations of indium
6 were measured using ICP-MS.

7
8 **Fig. 7** The levels of intracellular reactive oxygen species (ROS) in A549 cells exposed
9 ITO-DMEM-FBS dispersions. Cells were exposed to stable ITO-DMEM-FBS dispersions for
10 6, 24, and 72 h; then, we measured the intracellular ROS levels with the DCFH method, using
11 a flow cytometer. The value of the DCF fluorescence standardized untreated control was 1. *
12 $P < 0.05$, ** $P < 0.01$ (versus control, Dunnett, analysis of variance [ANOVA]).

13
14 **Fig. 8** The mRNA transcript levels of *HMOX-1* in A549 cells exposed ITO-DMEM-FBS
15 dispersions. The cells were exposed to stable ITO-DMEM-FBS dispersions for 24 and 72 h,
16 and then, we measured the expression levels of *HMOX-1* using real-time PCR. Each transcript
17 level was normalized to corresponding β -actin value and presented as relative units compared
18 to untreated control. * $P < 0.05$, ** $P < 0.01$ (versus control, Dunnett, analysis of variance
19 [ANOVA]).

1
2
3
4 1

5
6
7 2 **Fig. 9** Effect of indium tin oxide (ITO) NPs on DNA integrity. A549 cells were exposed to
8
9
10 3 stable ITO-DMEM-FBS dispersions for 24 and 72 h. The tail length values of DNA were
11
12 4 obtained by analyzing at least 50 random comet images from each treatment. The left panels
13
14
15 5 are comet images of untreated and ITO-exposed cells at 24 and 72 h. ** $P < 0.01$ (versus
16
17
18 6 control, Dunnett, analysis of variance [ANOVA]).
19

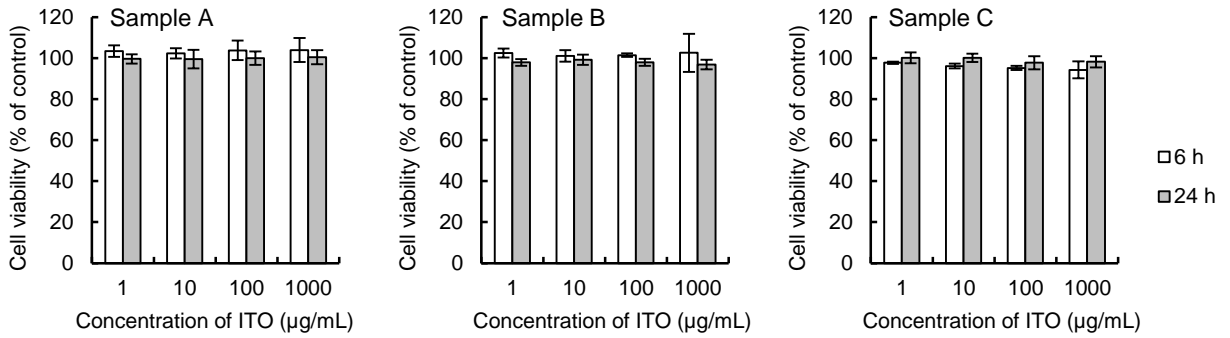
20
21 7
22
23

24 8 **Fig. 10** Clonogenic assays of cells exposed to stable ITO-DMEM-FBS medium dispersions.
25
26
27 9 A549 cells were treated with stable ITO-DMEM-FBS dispersions. Cell proliferation was
28
29
30 10 measured using the clonogenic assay. After the cells were cultured with the ITO-DMEM-FBS
31
32
33 11 dispersion for 7 days, the number of colonies were counted. Cell proliferation was
34
35
36 12 standardized to the untreated cells (100%). ** $P < 0.01$ (versus control, Dunnett, analysis of
37
38
39 13 variance [ANOVA]).
40

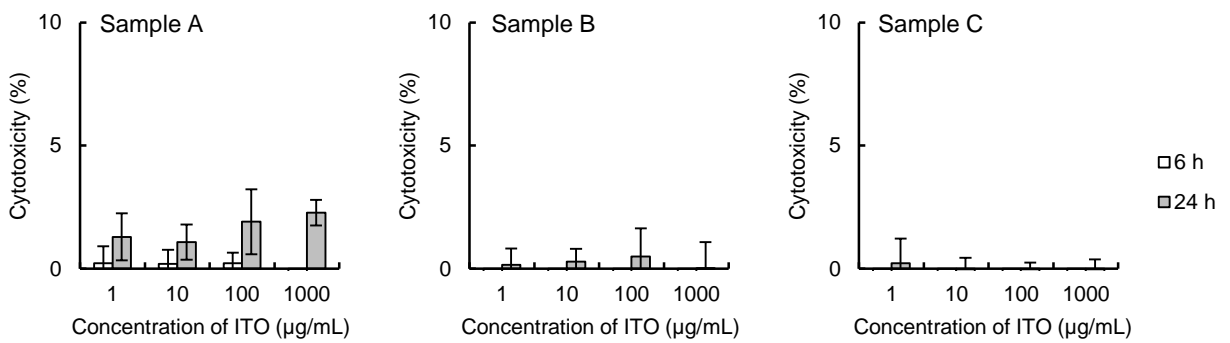
41 14
42
43
44
45
46
47
48
49
50
51
52
53
54
55
56
57
58
59
60

1
2
3
4
5
6
7
8
9
10
11
12
13
14
15
16
17
18
19
20
21
22
23
24
25
26
27
28
29
30
31
32
33
34
35
36
37
38
39
40
41
42
43
44
45
46
47
48
49
50
51
52
53
54
55
56
57
58
59
60

(A) WST-1 assay

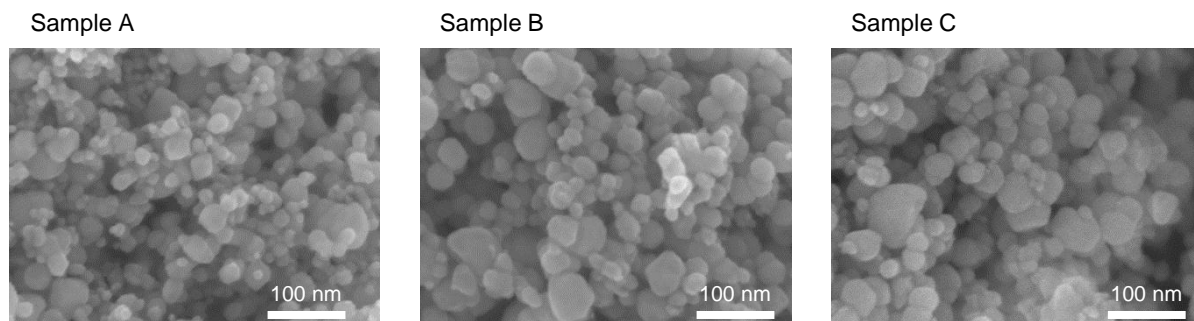


(B) LDH assay

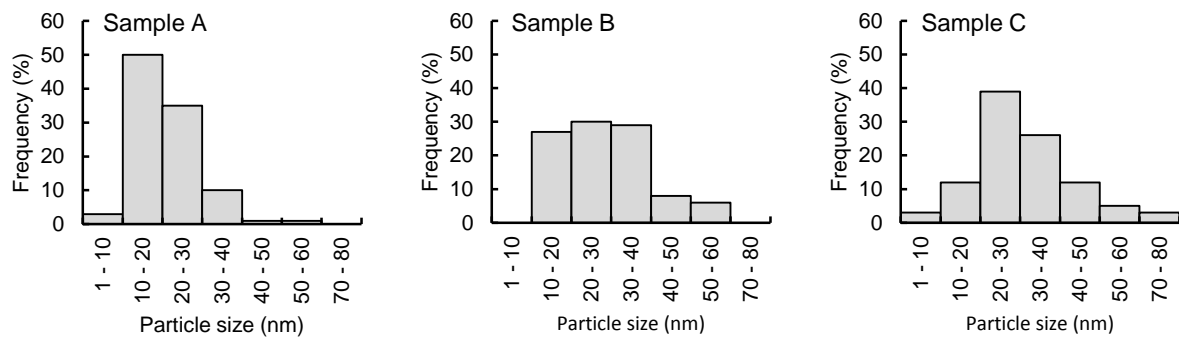


Metallomics Accepted Manuscript

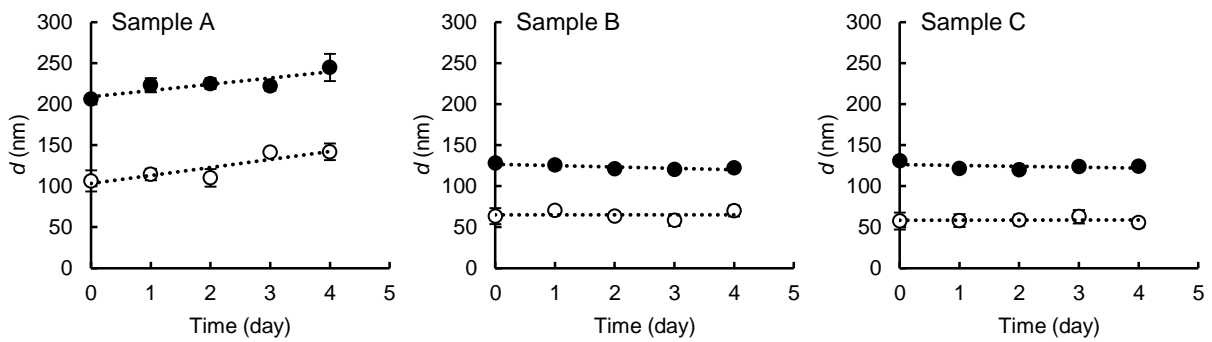
(A) FE-SEM



(B) Size distribution



(A) Secondary particle size



(B) Light scattering intensity

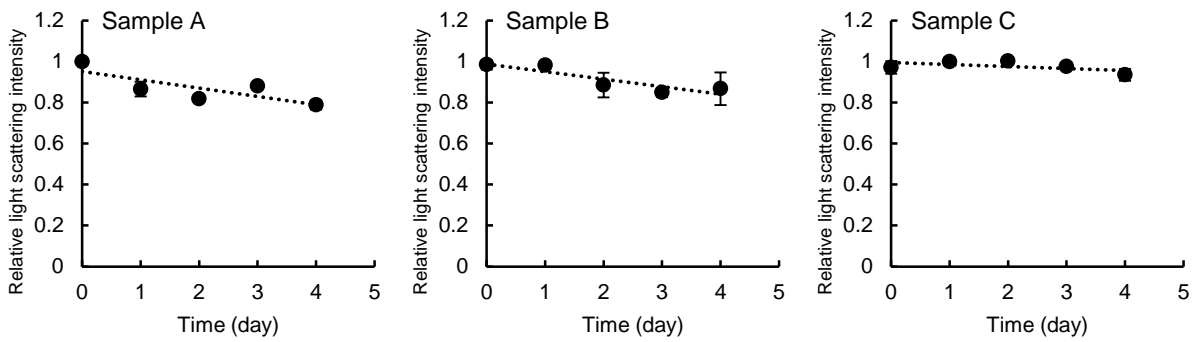
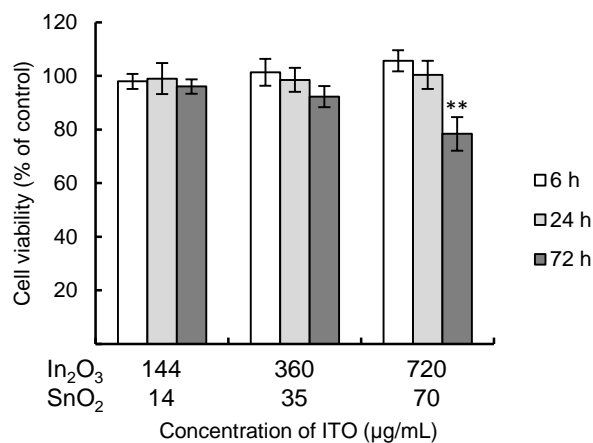
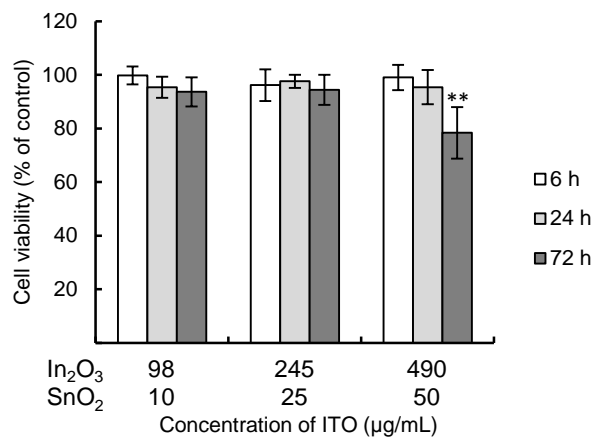


Figure 3

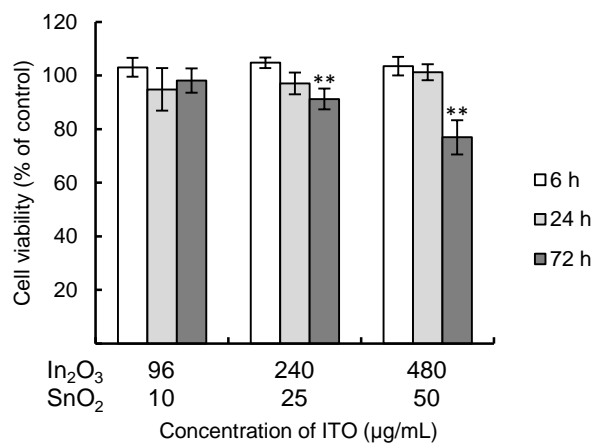
(A) Sample A



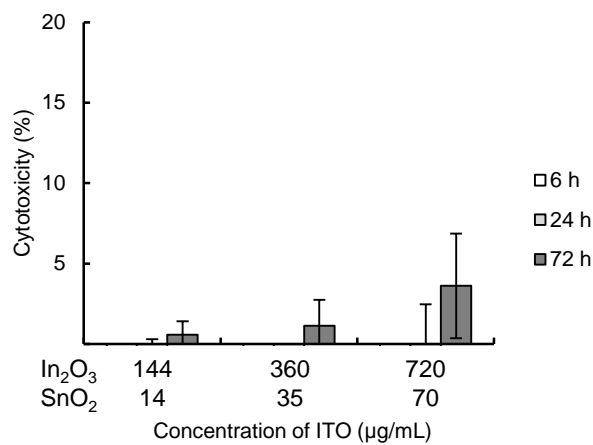
(B) Sample B



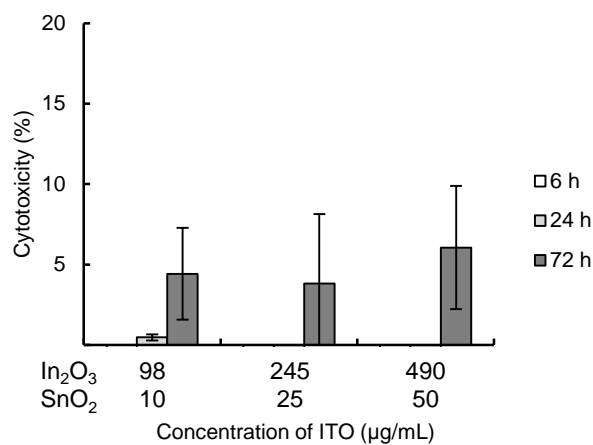
(C) Sample C



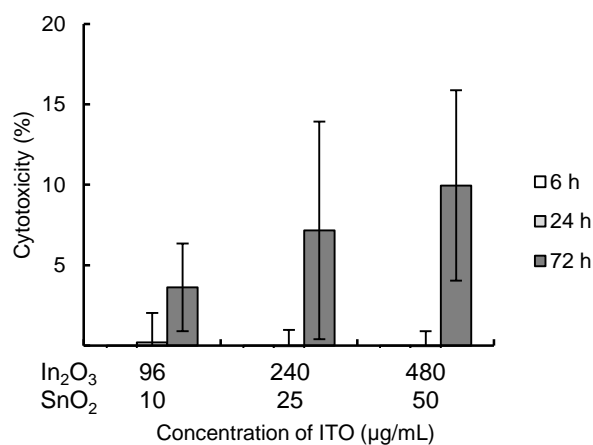
(A) Sample A



(B) Sample B

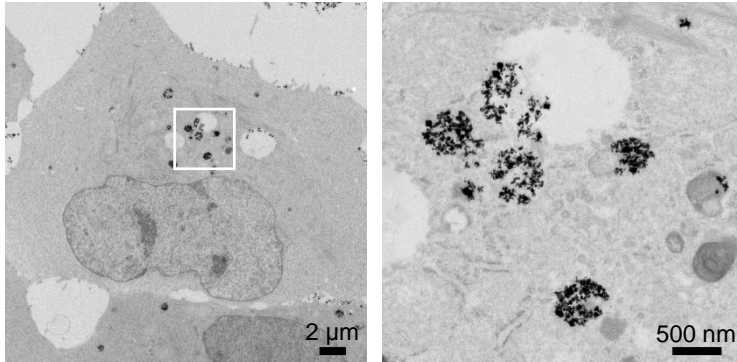


(C) Sample C

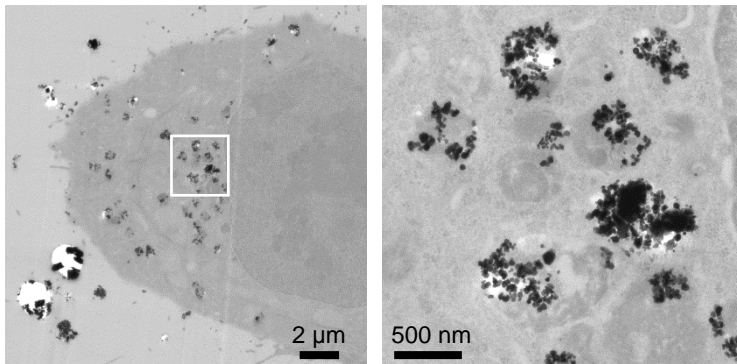


(A) TEM

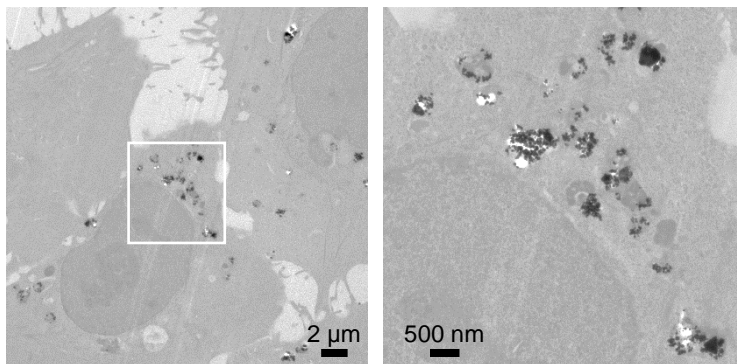
Sample A



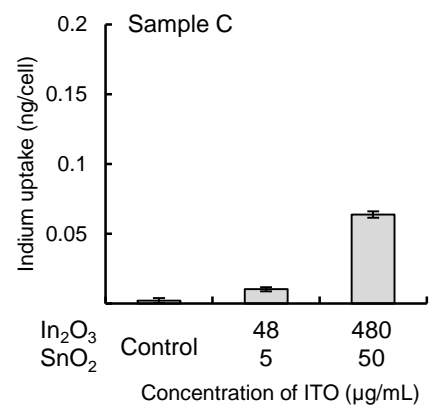
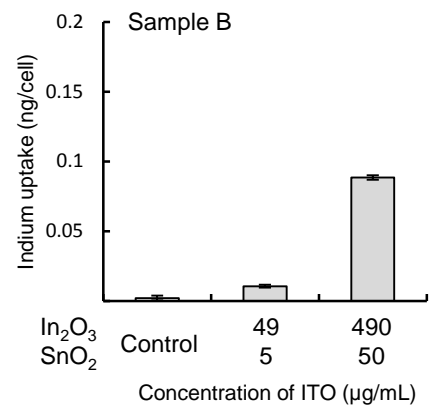
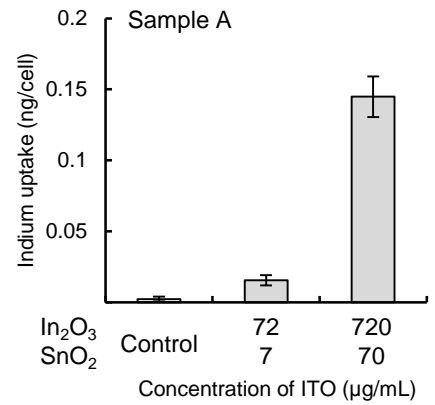
Sample B



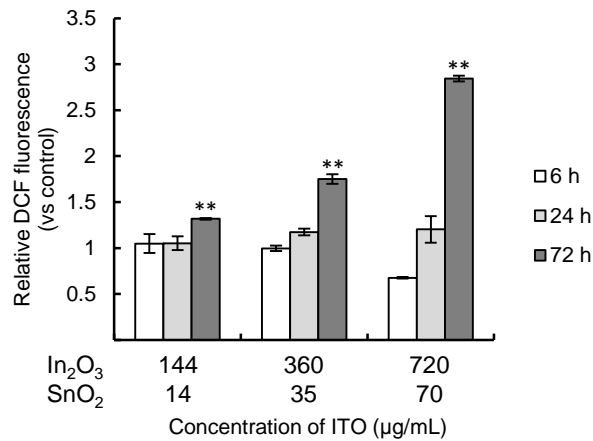
Sample C



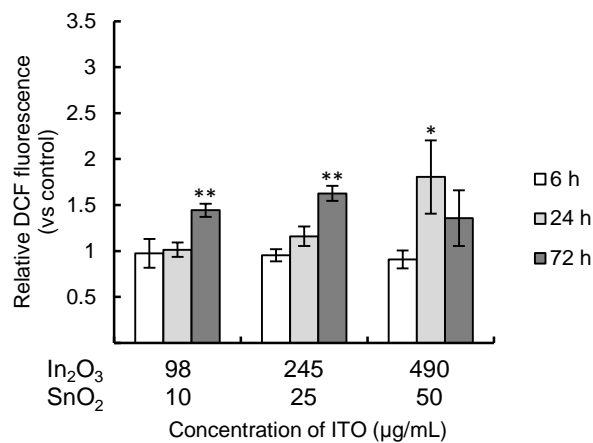
(B) Uptake of indium



(A) Sample A



(B) Sample B



(C) Sample C

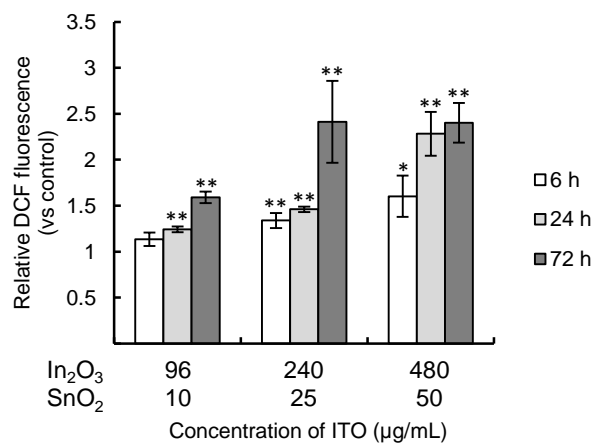
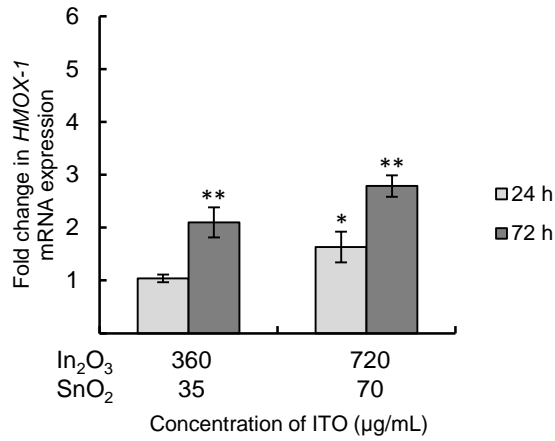
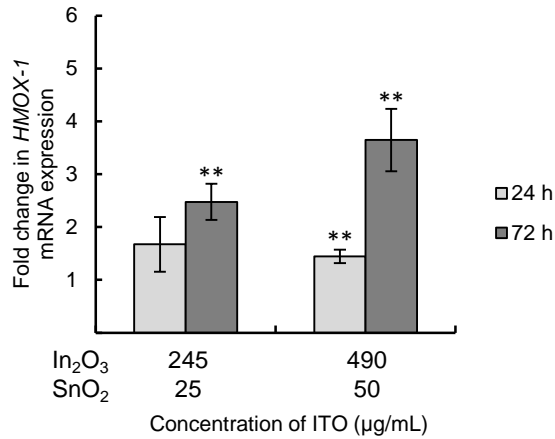


Figure 7

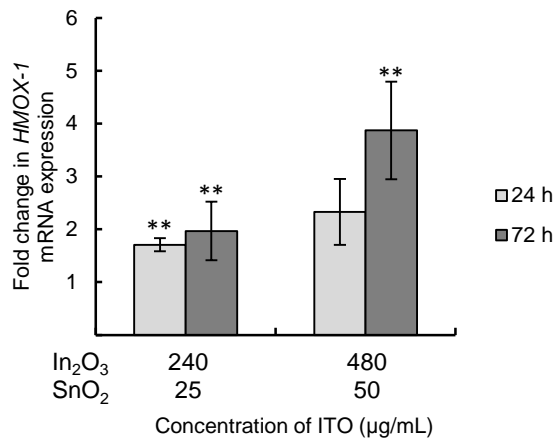
(A) Sample A

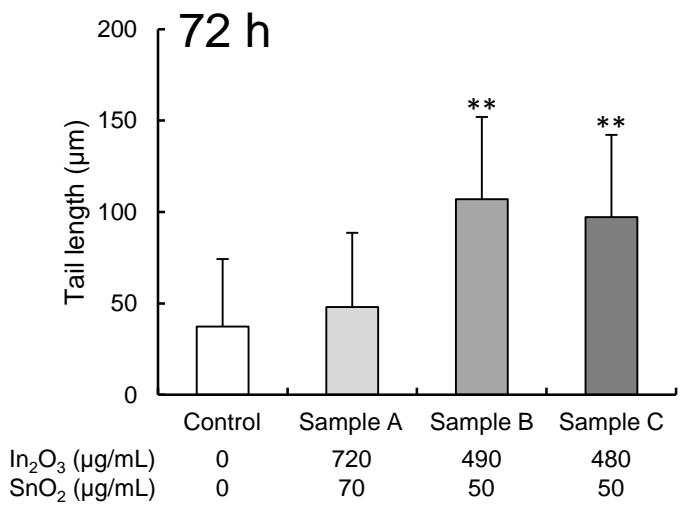
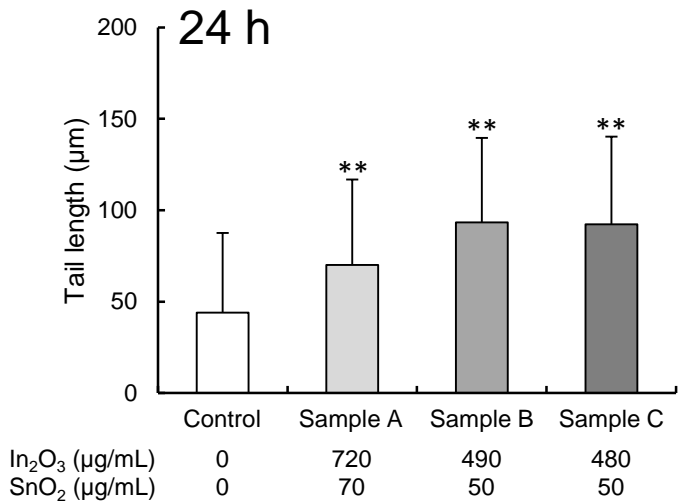
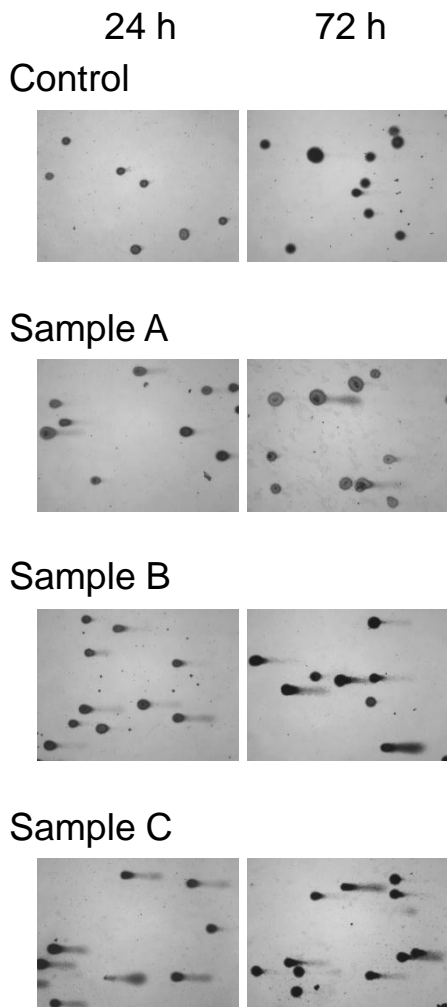


(B) Sample B



(C) Sample C

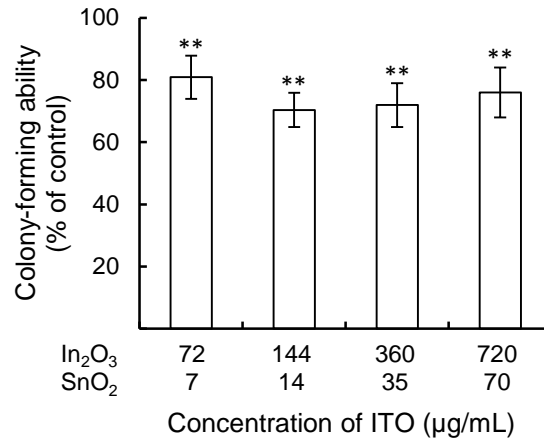




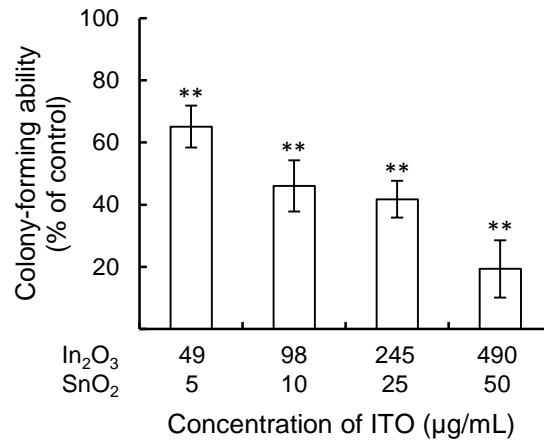
Metallomics Accepted Manuscript

Figure 9

(A) Sample A



(B) Sample B



(C) Sample C

